JOURNAL OF THEORETICAL
AND APPLIED MECHANICS
4, **39**, 2001

STABILITY AND LOAD-CARRYING CAPACITY OF THIN-WALLED ORTHOTROPIC POLES OF REGULAR POLYGONAL CROSS-SECTION SUBJECT TO COMBINED LOAD

MARIAN KRÓLAK
TOMASZ KUBIAK
ZBIGNIEW KOŁAKOWSKI

Department of Strength of Materials and Structures, Technical University of Łódź
e-mail: kola@orion.p.lodz.pl

Analysis of stability and load-carrying capacity of thin-wall orthotropic poles (columns, beams, masts, shafts) is conducted in the paper. The pole cross-section is a regular polygon and it is subjected to combined loads (compression, bending or torsion). The problem of buckling (stability problem) is solved using the asymptotic method by Byskov and Hutchinson with taking into account the second order approximation. Correctness of the results concerning the stability problem (critical loads and buckling modes) are verified by means of the finite element method using the programme ANSYS 5.4. FEM is also used in order to calculate load-carrying capacities. Numerical results are presented in diagrams. On the basis of the results several conclusions and final remarks are derived.

Key words: orthotropic pole, thin-walled structures, stability, load-carrying capacity

1. Introduction

The majority of hitherto published papers in the field of stability problems in thin-walled structures deals with buckling and post-buckling as well as load-carrying capacity of isotropic or orthotropic members like: plates, beams, columns and shells subjected to simple loads, particularly to uniform compression. Generally, problems of stability in thin-walled structures are so

complex, that even for simple cases like compression or shear, obtained solutions are usually of certain level of approximation and are derived using analytical, analytical-numerical or purely numerical methods. Several works, which had been published before 1995, concerning the stability, post-buckling in the elastic and elasto-plastic range as well as the load-carrying capacity of thin-walled girders subjected to either simple or combined load are widely discussed in two complete editions by Królak (1990, 1995).

A solution to the stability problem in thin-walled members (columns, beams, shafts) is extremely difficult when the member cross-section is of complex shape and the member is subjected to combined load. Because of complex buckling modes such a problem can not be solved using any analytical method. The most widely used and most general method which can be applied in that case is the finite element method since it enables one to calculate buckling and ultimate loads of thin-walled structures of different shapes, different boundary conditions and under an arbitrary system of loading. The second method, which has been used in the stability analysis for about 25 years, is a finite strips method. The method is particularly used in the analysis of girders of flat walls subjected to combined load (Plank and Wittrick, 1974a; Graves-Smith and Sridharan, 1978). It is also used in the analysis of the post-buckling state (Sridharan and Graves-Smith, 1981) and of the interactive buckling (Benito and Sridharan, 1985).

In the past, thin-walled structural members used to be made of isotropic materials mostly. Nowadays, carrying structural members are very often made of orthotropic composite materials, like fibrous cross-ply composites (fibres perpendicular to each other). One of the advantages of composite materials is a relatively wide range within which a designer can form their material properties in chosen directions or chosen areas. Particularly, material properties of composite orthotropic rectangular plates and also thin-walled bars (columns, beams, hollow shafts) of flat walls can be formed in an easy way. Designers who want to apply orthotropic, composite materials (of desirable strength properties) for carrying thin-walled members search for information about structural behaviour of such members subjected to different loads. In order to fulfil those requirements the stability problem of thin-walled orthotropic struts subject to combined loads is solved in the present paper. An analytical-numerical method of transition matrices is applied to the solution. The method was successfully used by several authors (Królak and Kołakowski, 1987; Biskupski and Kołakowski, 1994; Królak, 1995) in the analysis of global, local and also coupled buckling of structures subjected to simple loads.

Analytical-numerical methods, although less general than FEM, allow one

to generate equations and formulas with an analytical method, and then to obtain their solutions numerically. In comparison with pure numerical methods, their basic advantages are lower requirements as far as hardware is concerned and considerably shorter computational time. The correctness of the solution to the stability problem (critical loads and buckling modes) obtained with the analytical-numerical method has been verified with the finite element method (ANSYS 5.4).

2. Aim of the analysis

Carrying structural elements formed as thin-walled members (columns, beams, shafts) subjected to combined load are widely used in modern structures. More and more often, such members are made of orthotropic composite materials.

The aims of the present analysis are as follows:

- solution to the stability problem of thin-walled poles of closed cross-sections built of orthotropic flat walls and subjected to combined load
- elaboration of a computer programme
- realisation of numerical calculations of buckling loads of selected poles, using the programme mentioned above
- comparison of the obtained results with the results derived from the finite element method (using ANSYS 5.4)
- calculations of load-carrying capacities of analysed poles using FEM.

The applied analytical-numerical method allows us to calculate buckling loads and also buckling modes of thin-walled poles of different wall thickness. The material of each wall (strip) can have different properties.

3. Formulation of the problem and basic equations

Consider a thin-walled structural member (beam, column, shaft) of a prismatic cross-section and the length l which is built of orthotropic rectangular plates (walls) having principal directions of orthotropy parallel to their edges. The member cross-section can be either an open or closed (polygonal) profile with one axis of symmetry. Each column wall can be divided into several (less

than ten or a dozen or so) plate strips. Each strip as well as each wall can be of different thickness and made of different materials. Due to the applied orthogonalisation method by Godunov, see Bidermann (1977), the differences in the thicknesses and material properties of the adjacent walls (or plate strips) can be significant.

The considered thin-walled member is simply supported at the ends and can be subjected to a normal load and also to a bending moment. When the member is of a closed profile a constant torsional moment may be exerted upon it as well. The plate model of the structure is applied for the purposes of the stability analysis.

For the kth wall the following general non-linear geometric relations are taken into consideration

$$\begin{aligned}
\varepsilon_{xk} &= u_{k,x} + \frac{1}{2}(u_{k,x}^2 + v_{k,x}^2 + w_{k,x}^2) \\
\varepsilon_{yk} &= v_{k,y} + \frac{1}{2}(u_{k,y}^2 + v_{k,y}^2 + w_{k,y}^2) \\
\varepsilon_{xyk} &= \frac{1}{2}(u_{k,y} + v_{k,x} + u_{k,x}u_{k,y} + v_{k,x}v_{k,y} + w_{k,x}w_{k,y}) \\
\kappa_{xk} &= -w_{k,xx} \qquad \kappa_{yk} = -w_{k,yy} \qquad \kappa_{xyk} = -w_{k,xy}
\end{aligned} \tag{3.1}$$

Physical equations for the kth wall (strip) are as follows

$$\begin{aligned}
\varepsilon_{xk} &= \frac{1}{E_{xk}t_k}(N_{xk} - \nu_{xyk}N_{yk}) \qquad \varepsilon_{xyk} = \frac{1}{2G_k t_k}N_{xyk} \\
\varepsilon_{yk} &= \frac{1}{E_{yk}t_k}(N_{yk} - \nu_{yxk}N_{xk})
\end{aligned} \tag{3.2}$$

Elastic moduli and Poisson's ratios in equations (3.2) are related to each other in the following way

$$E_{xk}\nu_{yxk} = E_{yk}\nu_{xyk} \tag{3.3}$$

Variational equilibrium equations obtained from the principle of virtual works and corresponding to geometric equations (3.1) take the form

$$\int_S \left[N_{x,x} + N_{xy,y} + (N_x u_{,x})_{,x} + (N_y u_{,y})_{,y} + (N_{xy}u_{,x})_{,y} + (N_{xy}u_{,y})_{,x}\right] \delta u dS = 0$$

$$\int_S \left[N_{xy,x} + N_{y,y} + (N_x v_{,x})_{,x} + (N_y v_{,y})_{,y} + (N_{xy}v_{,x})_{,y} + (N_{xy}v_{,y})_{,x}\right] \delta v dS = 0$$

$$\int_S \Big[M_{x,xx} + M_{y,yy} + 2M_{xy,xy} + q + (N_x w_{,x})_{,x} + (N_y w_{,y})_{,y} + \tag{3.4}$$
$$+(N_{xy} w_{,x})_{,y} + (N_{xy} w_{,y})_{,x}\Big]\, \delta w dS = 0$$

where N_x, N_y and N_{xy} are the sectional forces and M_x, M_y, M_{xy} are the sectional moments.

Kinematic and static continuity conditions for junctions of the adjacent walls are described in the following form

$$\begin{aligned}
&u_{k+1} = u_k && w_{k+1} = w_k \cos\theta_k - v_k \sin\theta_k \\
&w_{k+1,y} = w_{k,y} && v_{k+1} = w_k \sin\theta_k + v_k \cos\theta_k \\
&M_{yk+1} = M_{yk} && N^*_{xyk+1} = N^*_{xyk} \\
&N^*_{yk+1} - N^*_{yk}\cos\theta_k - Q^*_{yk}\sin\theta_k = 0 && \\
&Q^*_{yk+1} - N^*_{yk}\sin\theta_k - Q^*_{yk}\cos\theta_k = 0 &&
\end{aligned} \tag{3.5}$$

where

$$\begin{aligned}
M_{yk} &= -D_{yk}(w_{k,yy} + \nu_{xyk} w_{k,xx}) \\
N^*_{yk} &= N_{yk} + N_{yk}\nu_{ky} + N_{xyk}\nu_{k,x} \\
Q^*_{yk} &= N_{yk} w_{k,y} + N_{xyk} w_{k,x} - D_{yk}[w_{k,yy} + (\nu_{xyk} + 4g_{yk}) w_{k,xxy}] \\
g_{yk} &= \frac{K_{sk}}{K_{yk}} = \frac{G_k(1 - \nu_{xyk}\nu_{yxk})}{E_{yk}}
\end{aligned} \tag{3.6}$$

Boundary conditions corresponding to simple supports of both ends of the member are fulfilled in the following way

$$\sum_{k=1}^{N} \frac{1}{b_k} \int_{y_k} N_{xk}\Big|_{x=0,y_k} dy_k = \sum_{k=1}^{N} \frac{1}{b_k} \int_{y_k} N_{xk}\Big|_{x=l,y_k} dy_k = \sum_{k=1}^{N} N^0_{xk}$$

$$\begin{aligned}
&v_k\Big|_{x=0,y_k} = v_k\Big|_{x=l,y_k} = 0 \\
&w_k\Big|_{x=0,y_k} = w_k\Big|_{x=l,y_k} = 0 \\
&M_{yk}\Big|_{x=0,y_k} = M_{yk}\Big|_{x=l,y_k} = 0
\end{aligned} \tag{3.7}$$

where b_k is the width of the kth wall or plate strip.

4. Solution to the problem

The stability problem (for the 1st order approximation) is solved using the asymptotic Koiter method (Królak, 1990, 1995). The displacement fields U and fields of the sectional forces N have been expanded in power series with respect to the amplitudes of the buckling modes ξ_n (ξ_n – amplitude of the nth buckling mode divided by the thickness t_1 of the column wall regarded as the first one)

$$\overline{U}_k = \lambda \overline{U}_k^{(0)} + \xi_n \overline{U}_k^{(n)} \qquad \overline{N}_k = \lambda \overline{N}_k^{(0)} + \xi_n \overline{N}_k^{(n)} \tag{4.1}$$

where $\overline{U}_k^{(0)}$ and $\overline{N}_k^{(0)}$ are the fields of the pre-buckling state while $U_k^{(n)}$ and $N_k^{(n)}$ are the fields corresponding to the nth buckling mode.

For a complex load the membrane forces of the pre-buckling state acting in the kth plate are taken as follows

$$N_{xk}^0 = E_{xk} t_k \varepsilon_{xk}^0 \qquad N_{yk}^0 = 0 \qquad N_{xyk}^0 = 2G_k t_k \varepsilon_{xyk}^0 \tag{4.2}$$

The displacements in the pre-buckling state for the assumed boundary conditions (support conditions at the member ends) are obtained in the form

$$u_k^0 = \varepsilon_{xk}^0 x \qquad v_k^0 = -\nu_{xyk}\varepsilon_{xk}^0 y_k + 2\varepsilon_{xyk}^0 x \tag{4.3}$$

Equilibrium equations expressed in terms of the displacements for the first order approximation are described as follows

$$\begin{aligned}
&u_{k,\xi\xi}^{(n)} + g_{xi} u_{k,\eta\eta}^{(n)} + (\nu_{yxk} + g_{xk}) v_{,\xi\eta}^{(n)} + (3 - \nu_{xyk}\nu_{yxk})\varepsilon_{xk}^0 u_{k,\xi\xi}^{(n)} + \\
&+4 g_{xk}\varepsilon_{xyk}^0 u_{k,\xi\eta}^{(n)} + 2 g_{xk}\varepsilon_{xk}^0 u_{k,\eta\eta}^{(0)} + 2\varepsilon_{xyk}^0 v_{k,\xi\xi}^{(n)} + \\
&+(1 - \nu_{xyk})(\nu_{yxk} + g_{xk})\varepsilon_{xk}^0 v_{k,\xi\eta}^{(n)} + 2 g_{xk}\varepsilon_{xyk}^0 v_{k,\eta\eta}^{(n)} = 0 \\
&(\nu_{xyk} + g_{yk}) u_{,\xi\eta}^{(n)} + g_{yk} v_{k,\xi\xi}^{(n)} + v_{k,\eta\eta}^{(n)} + (1 - \nu_{xyk})(\nu_{xyk} + g_{yk})\varepsilon_{xk}^0 u_{k,\xi\eta}^{(n)} + \\
&+\left(\frac{E_{xk}}{E_{yk}} - \nu_{xyk}^2 - 2\nu_{xyk} g_{yk}\right)\varepsilon_{xk}^0 v_{k,\xi\xi}^{(n)} + \\
&+4(\nu_{xyk} + 2 g_{yk})\varepsilon_{xyk}^0 v_{k,\xi\eta}^{(n)} - 2\nu_{xyk}\varepsilon_{xk}^0 v_{k,\eta\eta}^{(n)} = 0 \\
&w_{k,\xi\xi\xi\xi}^{(n)} + 2(\nu_{xyk} + 2 g_{yk}) w_{k,\xi\xi\eta\eta}^{(n)} + \frac{E_{yk}}{E_{xk}} w_{k,\eta\eta\eta\eta}^{(n)} - \\
&-12(1 - \nu_{xyk}\nu_{yxk})\left(\frac{b_k}{t_k}\right)^2 \varepsilon_{xk}^0 w_{k,\xi\xi}^{(n)} - 48\left(\frac{b_k}{t_k}\right)^2 g_{xk}\varepsilon_{xyk}^0 w_{k,\xi\eta}^{(n)} = 0
\end{aligned} \tag{4.4}$$

where

$$g_{xk} = \frac{K_{sk}}{K_{xk}} = \frac{G_k(1 - \nu_{xyk}\nu_{yxk})}{E_{xk}}$$

$$\xi = \frac{x}{b_k} \qquad \eta = \frac{y_k}{b_k}$$

In order to obtain a convergent numerical solution to the problem the following orthogonal functions of the first order fields (corresponding to boundary conditions at longitudinal edges) are introduced

$$\begin{aligned}
&\overline{a}_k^{(n)} = N_{yk}^{*(n)} \frac{b_k}{K_{yk}} = (1 + 2\nu_{xyk}\lambda\Delta_k)v_{k,\eta}^{(n)} + \nu_{xy}(1 + \nu_{xyk}\lambda\Delta_k - \lambda\Delta_k)u_{k,\xi}^{(n)} \\
&\overline{b}_k^{(n)} = N_{xyk}^{*(n)} \frac{b_k}{K_{xk}} = g_{xk}[(1 - 2\lambda\Delta_k)u_{k,\eta}^{(n)} + (1 + \nu_{xyk}\lambda\Delta_k - \lambda\Delta_k)v_{k,\xi}^{(n)}] \\
&\overline{c}_k^{(n)} = u_k^{(n)} \qquad\qquad \overline{d}_k^{(n)} = v_k^{(n)} \\
&\overline{e}_k^{(n)} = w_k^{(n)} \qquad\qquad \overline{f}_k^{(n)} = w_{k,\eta}^{(n)} \\
&\overline{g}_k^{(n)} = -M_{yk}^{(n)} \frac{b_k^2}{D_{yk}} = w_{k,\eta\eta}^{(n)} + \nu_{xyk} w_{k,\xi\xi}^{(n)} \\
&\overline{h}_k^{(n)} = -Q_{yk}^{*(n)} \frac{b_k^3}{D_{yk}} = w_{k,\eta\eta\eta}^{(n)} + (\nu_{xyk} + g_{yk}) w_{k,\xi\xi\eta}^{(n)}
\end{aligned} \tag{4.5}$$

where $(\cdot)_{k,\xi} = \partial(\cdot)/\partial\xi_k$, $(\cdot)_{k,\eta} = \partial(\cdot)/\partial\eta_k$.

Finally, the following system of differential equations is obtained

$$\begin{aligned}
&\overline{a}_{k,\eta}^{(n)} = -\Big[g_{yk} - \Big(\frac{E_{xk}}{E_{yk}} - \nu_{xyk}^2 - 2\nu_{xyk}g_{yk}\Big)\lambda\Delta_k\Big]\overline{d}_{k,\xi\xi}^{(n)} - \\
&\qquad -g_{yk}[1 - (1 - \nu_{xyk})\lambda\Delta_k]\overline{c}_{k,\xi\eta}^{(n)} \\
&\overline{b}_{k,\eta}^{(n)} = -[1 - (3 - \nu_{xyk}\nu_{yxk})\lambda\Delta_k]\overline{c}_{k,\xi\xi}^{(n)} - \nu_{yxk}[1 - (1 - \nu_{xyk})\lambda\Delta_k]\overline{d}_{k,\xi\eta}^{(n)} \\
&\overline{c}_{k,\eta}^{(n)} = \Big[\frac{\overline{b}_k^{(n)}}{g_{xk}} - (1 + \nu_{xyk}\lambda\Delta_k - \lambda\Delta_k)\overline{d}_{k,\xi}^{(n)}\Big](1 + 2\lambda\Delta_k)^{-1} \\
&\overline{d}_{k,\eta}^{(n)} = \Big[\overline{a}_k^{(n)} - \nu_{xyk}(1 + \nu_{xyk}\lambda\Delta_k - \lambda\Delta_k)\overline{c}_{k,\xi}^{(n)}\Big](1 + 2\nu_{xyk}\lambda\Delta_k)^{-1} \\
&\overline{e}_{k,\eta}^{(n)} = \overline{f}_k^{(n)} \qquad\qquad \overline{f}_{k,\eta}^{(n)} = \overline{g}_k^{(n)} - \nu_{xyk}\overline{e}_{k,\xi\xi}^{(n)} \\
&\overline{g}_{k,\eta}^{(n)} = \overline{h}_k^{(n)} - 4g_{yk}\overline{f}_{k,\xi\xi}^{(n)}
\end{aligned} \tag{4.6}$$

$$\overline{h}_{k,\eta}^{(n)} = -\frac{E_{xk}}{E_{yk}}\left[\nu_{yxk}\overline{f}_{k,\xi\xi\eta}^{(n)} + \overline{e}_{k,\xi\xi\xi\xi}^{(n)} + 12(1-\nu_{xyk}\nu_{yxk})\left(\frac{b_k}{t_k}\right)^2 \lambda \Delta_k \overline{e}_{k,\xi\xi}^{(n)}\right]$$

Solution to the system (4.6) was foreseen as

$$\begin{aligned}
\overline{a}_k^{(n)} &= \sum_m \overline{A}_{mk}^{(n)}(\eta_k)\sin\frac{m\pi b}{l}\xi & \overline{b}_k^{(n)} &= \sum_m \overline{B}_{mk}^{(n)}(\eta_k)\cos\frac{m\pi b}{l}\xi \\
\overline{c}_k^{(n)} &= \sum_m \overline{C}_{mk}^{(n)}(\eta_k)\cos\frac{m\pi b}{l}\xi & \overline{d}_k^{(n)} &= \sum_m \overline{D}_{mk}^{(n)}(\eta_k)\sin\frac{m\pi b}{l}\xi \\
\overline{e}_k^{(n)} &= \sum_m \overline{E}_{mk}^{(n)}(\eta_k)\sin\frac{m\pi b}{l}\xi & \overline{f}_k^{(n)} &= \sum_m \overline{F}_{mk}^{(n)}(\eta_k)\sin\frac{m\pi b}{l}\xi \\
\overline{g}_k^{(n)} &= \sum_m \overline{G}_{mk}^{(n)}(\eta_k)\sin\frac{m\pi b}{l}\xi & \overline{H}_k^{(n)} &= \sum_m \overline{H}_{mk}^{(n)}(\eta_k)\sin\frac{m\pi b}{l}\xi
\end{aligned} \tag{4.7}$$

After substituting the forecast functions given in (4.7) into equations (4.6) and applying the Kantorowich method (which was necessary to apply because of the difference in trigonometric functions in x directions) a system of ordinary differential equations is obtained where the unknown functions are $A_{mk} - H_{mk}$ (mth harmonic function of η_k). These functions will be determined using the numerical method of transition matrices after numerical integration of the equilibrium equations in the circumferential direction with respect to η_k (applying the Runge-Kutta procedure realised) in order to obtain a relation between the state vectors at the two longitudinal edges. The integration of the equilibrium equations was carried out using the Godunov orthogonalization method.

5. Abilities of the elaborated computer programme

The stability equations derived in Sections 3 and 4 with the co-operation conditions of the adjacent strips and with the assumed boundary conditions can only be solved numerically. Therefore, a computer procedure, in which it has been assumed that each strip can have various width, thickness and other material properties, has been developed. The external load acting on each strip can be different as well. Owing to this program, the stability of thin-walled structures with various shapes of the cross-section, wall (strip) thickness and material properties of the orthotropic strips – for the assumed structural loads (compression, bending, torsion) – can be calculated. Longitudinal stiffeners can be modelled with narrow plate strips.

6. Analysis of results of stability calculations

The first calculations were carried out using an analytical-numerical method. Buckling loads were calculated for a thin-walled pole with a regular octagonal cross-section subjected to bending and torsion and also to compression and torsion.

The plane of the pole in which the bending occurs is shown in Figure 1.

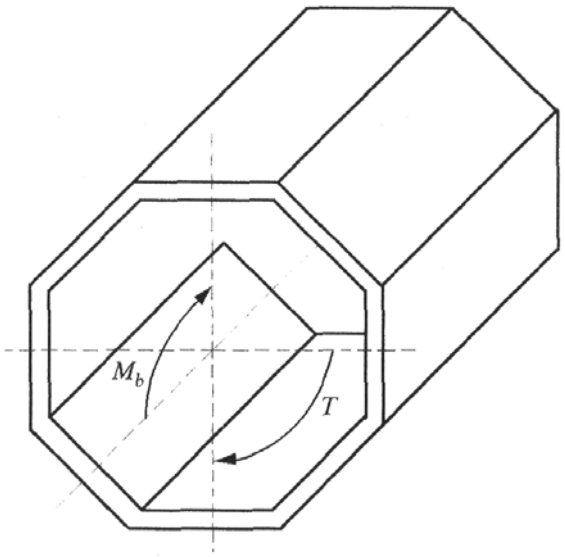

Fig. 1. Cross-section and loading of analysed thin-walled poles

Geometrical dimensions of the pole were as follows:
- length $l = 100$ mm (distance between diaphragms),
- wall width $b = 39.27$ mm,
- wall thickness (the same for all walls) $t = 1$ mm.

The calculations were conducted for three poles built of walls which were made of materials of the two following orthotropy ratios: $\eta = E_y/E_x = 3.2992$; $\eta = 1.0$ (isotropy); $\eta = 0.3031$.

The dimensionless values of buckling stresses

$$\sigma^*_{b\,cr} = \frac{\sigma_{b\,cr}10^3}{E_x} \qquad \sigma^*_{c\,cr} = \frac{\sigma_{c\,cr}10^3}{E_x} \qquad \tau^*_{b\,cr} = \frac{\tau_{t\,cr}10^3}{E_x}$$

for different contributions of the bending and torsion in the total load expressed by σ_b/τ_t ratio are given in Table 1, while for different contributions of the compression and torsion – expressed by σ_0/τ_t – are given in Table 2 and are also presented in Figure 2.

Table 1

σ_b/τ_t	$\eta = 2.2992$		$\eta = 1$		$\eta = 0.3031$	
	$\sigma^*_{b\,cr}$	$\tau^*_{t\,cr}$	$\sigma^*_{b\,cr}$	$\tau^*_{t\,cr}$	$\sigma^*_{b\,cr}$	$\tau^*_{t\,cr}$
0	0	6.160	0	3.490	0	1.271
0.2	1.114	5.572	0.643	3.215	0.236	1.180
0.4	1.925	4.813	1.154	2.885	0.433	1.084
0.6	2.495	4.162	1.547	2.578	0.597	0.996
0.8	2.908	3.636	1.846	2.307	0.734	0.918
1.0	3.189	3.189	2.063	2.063	0.844	0.844
1.25	3.441	2.753	2.261	1.809	0.955	0.764
1.667	3.700	2.220	2.469	1.481	1.089	0.653
2.5	3.938	1.575	2.665	1.066	1.234	0.493
5.0	4.111	0.822	2.811	0.562	1.353	0.270
∞	4.174	0	2.865	0	1.399	0

Table 2

σ_b/τ_t	$\eta = 2.2992$		$\eta = 1$		$\eta = 0.3031$	
	$\sigma^*_{c\,cr}$	$\tau^*_{t\,cr}$	$\sigma^*_{c\,cr}$	$\tau^*_{t\,cr}$	$\sigma^*_{c\,cr}$	$\tau^*_{t\,cr}$
0	0	6.160	0	3.490	0	1.271
0.2	1.034	5.172	0.603	3.015	0.243	1.217
0.4	1.735	4.338	1.048	2.620	0.443	1.108
0.6	2.200	3.666	1.376	2.294	0.607	1.013
0.8	2.512	3.140	1.620	2.025	0.630	0.788
1.0	2.728	2.728	1.802	1.802	0.709	0.709
1.25	2.914	2.331	1.970	1.576	0.783	0.626
1.667	3.042	1.825	2.155	1.293	0.868	0.520
2.5	3.149	1.259	2.317	0.926	0.957	0.383
5.0	3.221	0.644	2.383	0.476	1.036	0.207
∞	3.246	0	2.407	0	1.070	0

In order to verify the results obtained using the elaborated computer programme the FEM programme ANSYS 5.4 has been applied.

The load carrying capacity of bent and torsionally deflected beam-columns has been determined with the finite element method as well. The applied program of the finite element method allows one to analyse:

- linear problem of stability (eigenvalue method), in which critical loads (bifurcation points) and buckling modes are determined
- non-linear problem of stability, in which the behaviour of the structure

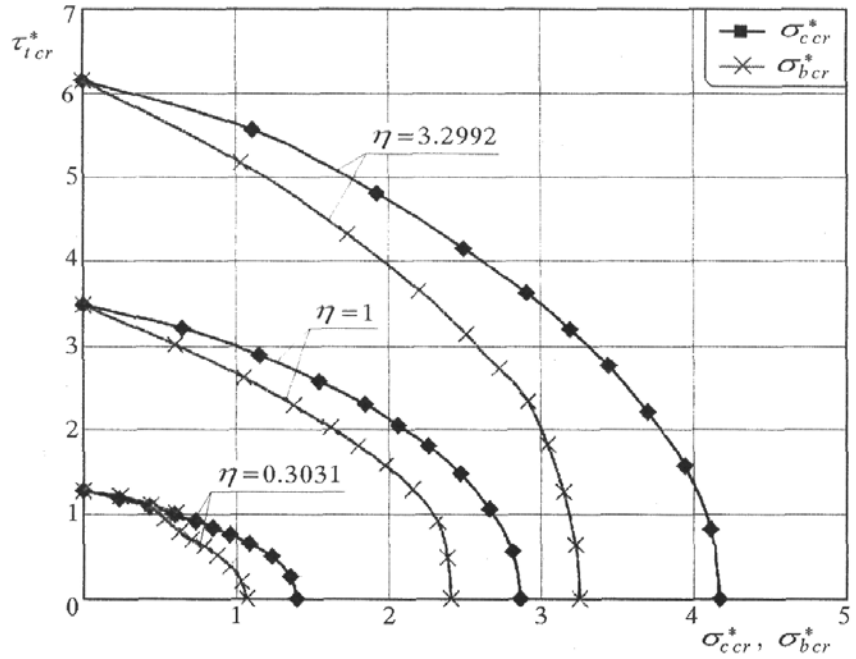

Fig. 2. Dimensionless values of the critical stress for different bending-to-torsion ratios

after the loss of stability is analysed and the load carrying capacity is determined.

The girder has been modelled with four-node shell elements with six degrees of freedom in each node. The load was realised by respective application of forces with distribution corresponding to bending and torsion.

The problem has been solved in two stages. In the first step, a linear analysis of the stability (eigenvalue method) has been carried out and, as a result, the buckling modes of the analysed girder and the critical values of loading have been determined.

In the second stage, a non-linear analysis of the stability, in which the non-linear equations have been solved by means of the Newton-Raphson method, has been carried out. A technique that allows for a non-linear analysis by a gradual increase in the loading has been employed. The analysis was possible owing to application of a special "arc-length" technique. This technique makes it possible to analyse the non-linear stability problem of a structure. In order to conduct such an analysis, the model should be prepared before, i.e. in the case when the loading does not cause a deflection that exerts an influence on the mode of the stability loss (e.g. a compressed plate), it is necessary to impose initial imperfections by modification of the geometry of the model so

that it has initial deflections whose value is equal to approximately 1/50 of the plate thickness, which corresponds to the lowest buckling mode. In the case when the way the load is applied causes the structure deflection (e.g. a rod being bent), the above described way of the model modification is not necessary.

Table 3 and Figure 3 present values of dimensionless buckling stresses in the analysed thin-walled pole of the regular octagonal cross-section made of am orthotropic material of following properties: $E_x = 29523\,\text{MPa}$, $E_y = 97423\,\text{MPa}$, $\eta = 3.2992$, $\nu_{yx} = 0.3$, $\nu_{xy} = 0.09$, $G = 11818\,\text{MPa}$. The presented values have been obtained using both analytical-numerical and finite element methods.

Table 3

σ_b/τ_t	Author's software		ANSYS 5.4			
	$\sigma^*_{b\,cr}$	$\tau^*_{t\,cr}$	$\sigma^*_{b\,cr}$	$\tau^*_{t\,cr}$	$M_{b\,cr}$ [Nm]	T_{cr} [Nm]
0	0	6.160	0	5.995	0	2641.9
0.2	1.114	5.572	1.118	5.555	255.2	2437.8
0.4	1.925	4.813	1.931	4.810	441.7	2109.0
0.6	2.495	4.162	2.473	4.098	568.1	1808.5
0.8	2.908	3.636	2.845	3.557	655.4	1564.7
1.0	3.189	3.189	3.116	3.116	715.3	1366.6
1.25	3.441	2.753	3.319	2.642	762.8	1165.6
1.667	3.700	2.220	3.486	2.100	804.4	921.8
2.5	3.938	1.575	3.658	1.456	840.0	641.8
5.0	4.111	0.822	3.760	0.745	863.7	330.0
∞	4.174	0	3.794	0	872.7	0

The given results indicate that the greatest divergence occurs for lower contribution of the torsional load – its highest value is about 10%. The reason for such a divergence may be a difficulty in exact modelling of the boundary conditions corresponding to both considered support conditions for the pole edges.

In Figure 4 the buckling modes of the pole walls are presented for $\sigma_b/\tau_t = 0$ (pure torsion) and $\tau_t/\sigma_b = 0$ (pure bending).

In the next phase the calculations of the buckling state were conducted for thin-walled poles of the length $l = 100\,\text{mm}$, the cross-section of which was a regular polygon with the number of sides equal to $N = 4, 6, 8, 12, 16$ and 20. The circumference of each of the considered polygons was the same and equal to the circumference of a circle of the radius $R = 50\,\text{mm}$. Thus, the width of

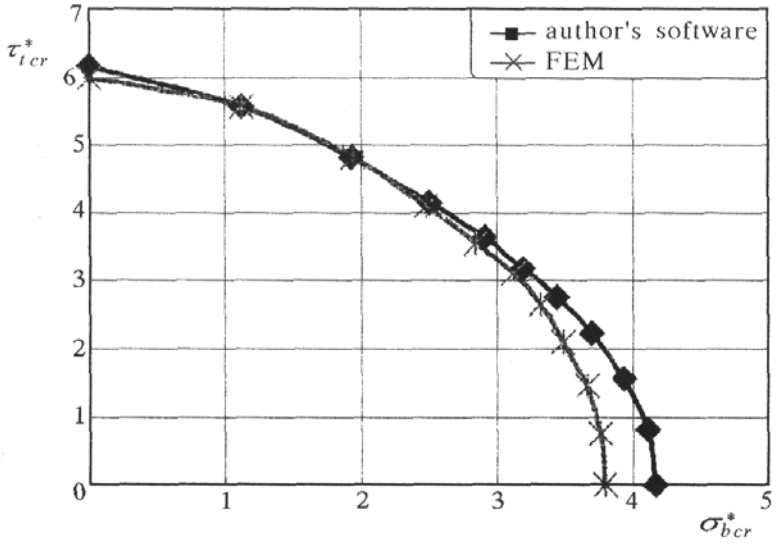

Fig. 3. Comparison of the results obtained by authors, software and by FEM

the wall of the polyhedron with N walls is determined as

$$b = \frac{2\pi R}{N}$$

Since the thickness of the polyhedron walls was considered to be the same for each wall and equal to $t = 1\,\text{mm}$, the area of the cross-section of each considered pole was the same.

The aim of the calculations was the analysis of the influence of the number of polygon sides (from a square up to a polygon of 20 sides) upon buckling stresses in the pole subjected to bending and torsion. The second aim was the verification of the correctness of the derived equations, the applied method of the solution of the problem and also the elaborated computer programme. The verification consisted in the comparison of the calculation results obtained for the isotropic thin-walled pole of the regular polygonal cross-section with the results known from the literature concerning isotropic cylindrical shell of the same length, thickness and circumference.

Thus, according to the results published by Sturm (1947) a cylindrical shell of dimensions: $l = 100\,\text{mm}$, $R = 50\,\text{mm}$ and $t = 1\,\text{mm}$, made of an isotropic material with Poisson's ratio $\nu = 0.3$ and subjected to torsion, buckles at the critical stress of the dimensionless value

$$\tau^*_{t\,cr} = \frac{\tau_{t\,cr} 10^3}{E_x} = 4.67$$

when the number n of halfwaves of the buckling amounts 6.

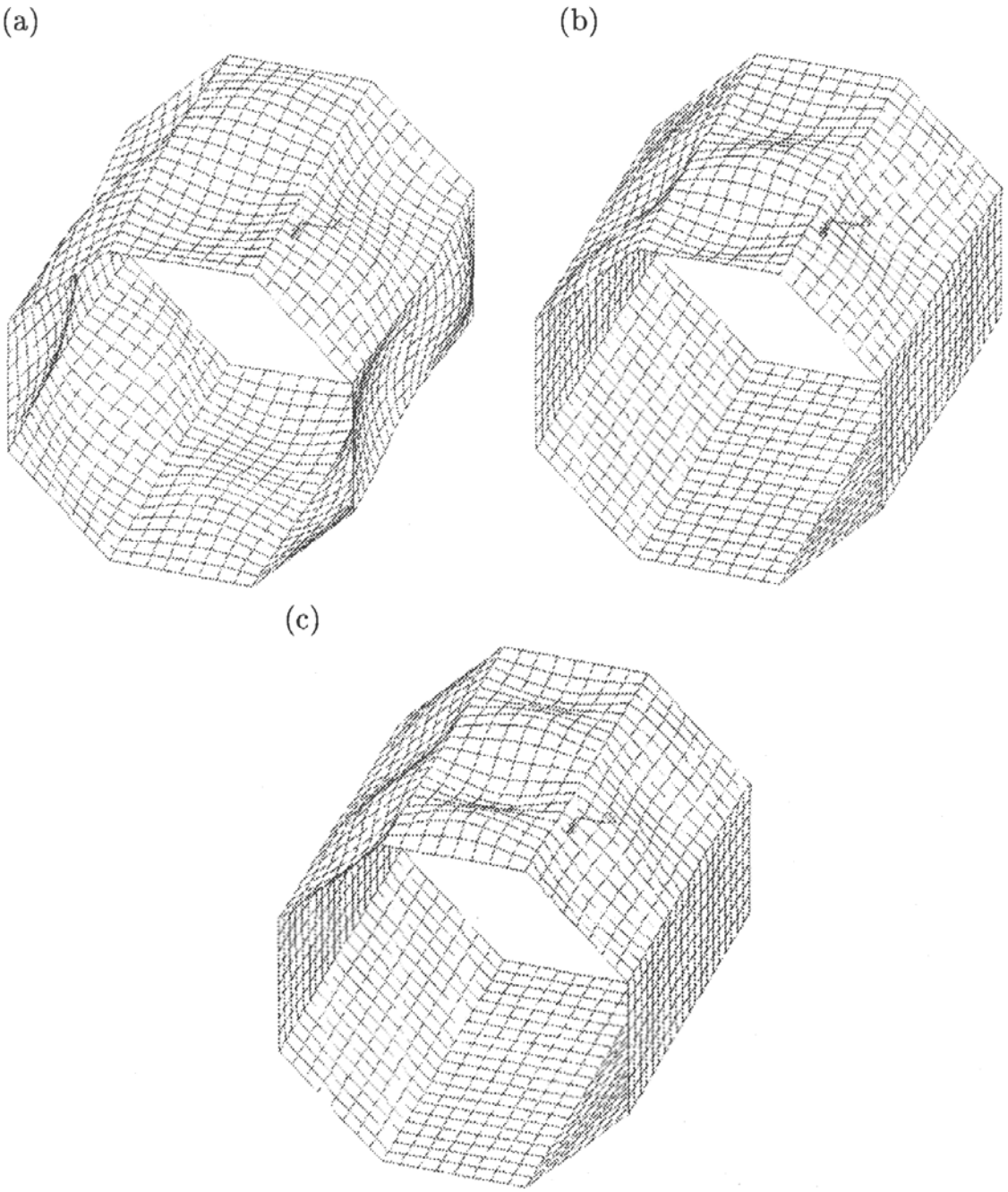

Fig. 4. Shape of the local buckling mode; (a) pure torsion $\sigma_b/\tau_t = 0$, (b) $\sigma_b/\tau_t = 1$, (c) pure bending $\tau_t/\sigma_b = 0$

The same cylindrical shell subject to pure bending buckles at the maximum dimensionless bending stress, which according

$$\sigma^*_{b\,cr} = \frac{\sigma_{b\,cr} 10^3}{E_x} = 12.1$$

Figure 5 presents diagrams of dimensionless buckling stresses in isotropic thin-walled poles of regular polygonal cross-sections $(N = 4, 6, 8, 12, 16, 20)$ subjected to bending and torsion.

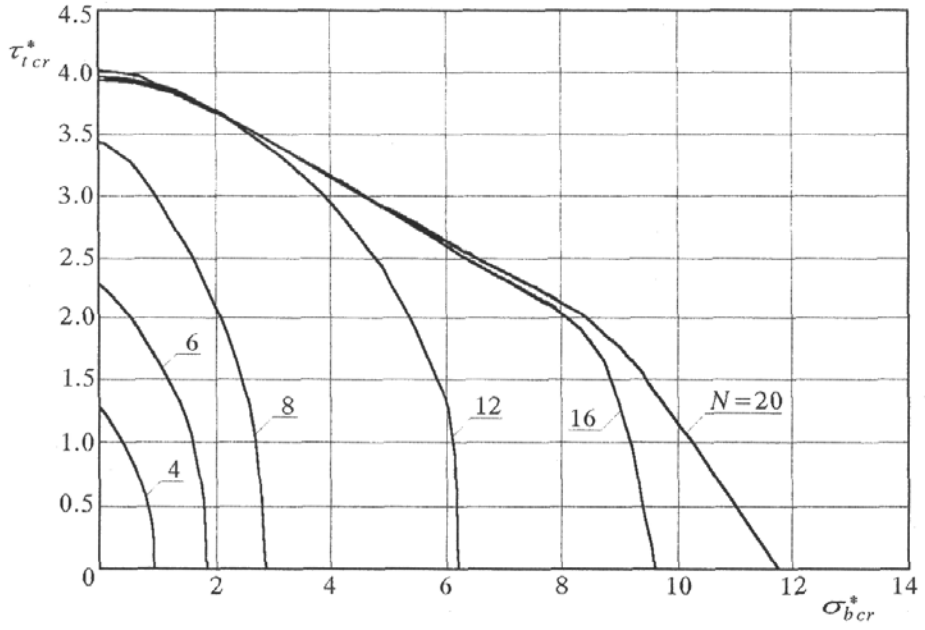

Fig. 5. Influence of the number of regular polygon sides on the stability of poles subject to torsion and bending

The dimensionless buckling stress $\sigma^*_{b\,cr}$ in the pole of the cross-section being the regular polygon of 20 sides, which is subject to pure bending, is about 3% lower than the corresponding buckling stress in the cylindrical shell under pure bending, which is mentioned above.

The comparison of the dimensionless buckling shear stresses in a cylindrical shell under torsion and the corresponding pole of the cross-section being a polygon of greater number of sides $(N = 12, 16, 20)$ shows that for $N \geqslant 12$ the buckling shear stresses are in the interval

$$3.93 \leqslant \tau^*_{t\,cr} \leqslant 4.67$$

and depend on the buckling mode (on the number of halfwaves in the circumferencial direction). For $N = 4 \div 16$ the number of halfwaves in the

circumferencial direction is equal to the number of walls (sides of the polygon) and for $N = 20$ it amounts 12, which corresponds to 6 halfwaves, like in the cylindrical shell.

The increase of the dimensionless buckling stresses related to the increase of the number N of the pole walls when under pure bending, is induced not only by the increase of the pole height (second moment of inertia of the cross-section) in the plane of bending but (may be to greater extend) diminution of the width of the pole walls as well.

In order to illustrate the post-buckling behaviour of thin-walled poles subjected to torsion and bending as well as in order to evaluate their load-carrying capacity numerical calculations were carried out using the programme ANSYS 5.4. The calculations were conducted for a pole of the following dimensions and material properties: $l = 100\,\text{mm}$, $b = 39.27\,\text{mm}$, $t = 1\,\text{mm}$, $E_x = 29523\,\text{MPa}$, $E_y = 97423\,\text{MPa}$, $G = 11818\,\text{MPa}$, $\nu_{yx} = 0.3$, $\nu_{xy} = 0.09$. Linear material behaviour of the pole was assumed. The values of buckling stresses in this pole are given in Table 3. The results of load-carrying capacity calculations are presented in Table 4 and also shown in Figure 6.

Table 4

$\eta = 1$												
σ_b/τ_t	N=4		N=6		N=8		N=12		N=16		N=20	
	$\sigma^*_{b\,cr}$	$\tau^*_{t\,cr}$	$\sigma^*_{b\,cr}$	$\tau^*_{t\,cr}$	$\sigma^*_{b\,cr}$	$\tau^*_{t\,cr}$	$\sigma^*_{b\,cr}$	$\tau^*_{t\,cr}$	$\sigma^*_{b\,cr}$	$\tau^*_{t\,cr}$	$\sigma^*_{b\,cr}$	$\tau^*_{t\,cr}$
0	0	1.287	0	2.287	0	3.490	0	3.930	0	4.039	0	3.971
0.2	0.231	1.158	0.419	2.098	0.643	3.215	0.778	3.890	0.786	3.932	0.778	3.891
0.4	0.404	1.011	0.753	1.833	1.154	2.885	1.512	3.780	1.512	3.781	1.500	3.750
0.6	0.531	0.885	1.011	1.685	1.547	2.578	2.175	3.626	2.176	3.627	2.162	3.603
0.8	0.624	0.780	1.206	1.508	1.846	2.307	2.758	3.447	2.782	3.478	2.769	3.461
1.0	0.693	0.693	1.352	1.352	2.063	2.063	3.259	3.259	3.335	3.335	3.325	3.325
1.25	0.754	0.603	1.481	1.185	2.261	1.809	3.783	3.027	3.962	3.169	3.958	3.167
1.667	0.819	0.491	1.614	0.968	2.469	1.481	4.447	2.668	4.867	2.920	4.880	2.928
2.5	0.879	0.351	1.733	0.693	2.665	1.066	5.249	2.099	6.275	2.510	6.397	2.535
5.0	0.923	0.184	1.816	0.363	2.811	0.562	6.033	1.206	8.663	1.732	8.936	1.787
∞	0.939	0	1.846	0	2.865	0	6.195	0	9.669	0	11.741	0

In the last column of Table 4 the number of halfwaves along the pole length is given for the wall which is most deformed at buckling.

For one of the considered loading modes when the stresses increase proportionally with the ratio $\sigma_b/\tau_t = 1$ the presented diagrams illustrate a simultaneous increase of bending moment in terms of the angular displacement of the cross-section and the torsional moment in terms of the angle of twist (Fig. 7). The maximum values of these curves indicate the load-carrying capa-

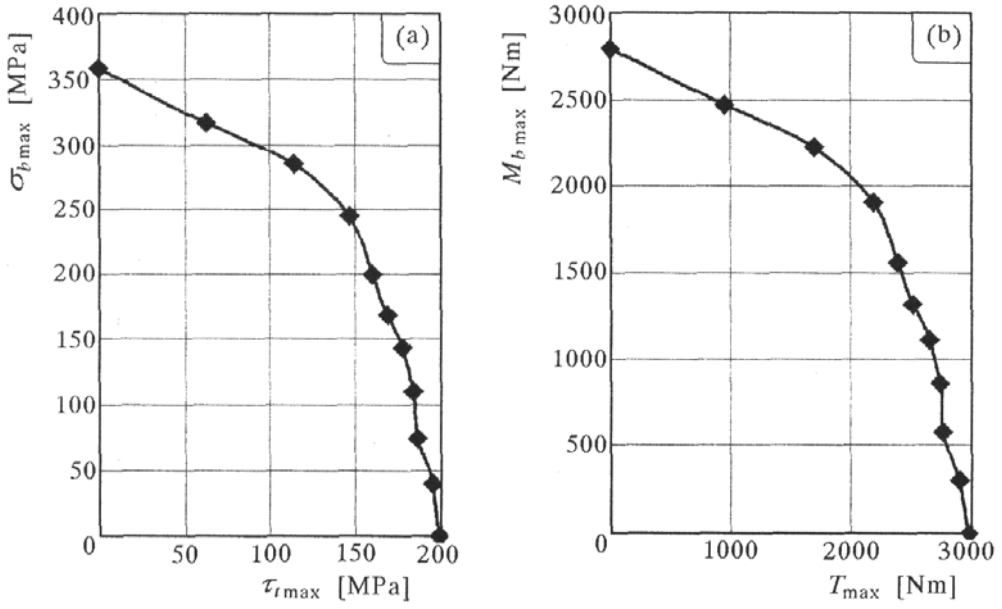

Fig. 6. Load carrying capacity of the thin-walled pole subject to bending and torsion for different torsion-to-bending ratios; (a) relation between moments, (b) relation between stresses

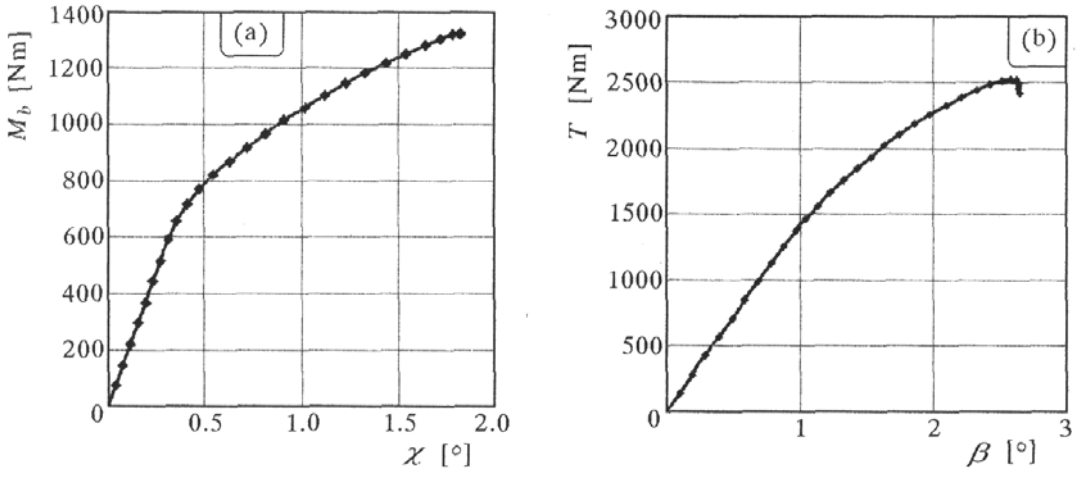

Fig. 7. Loading versus rotation angle curves; (a) bending moment versus rotation angle, (b) torsional moment versus rotation angle

city of the pole in the elastic range. These values are also presented in Table 5 ($\sigma_{\max} = \tau_{\max} = 169\,\text{MPa}$, $M_{b\ \max} = 2315\,\text{Nm}$, $T_{\max} = 1316\,\text{Nm}$). The values of $M_{b\ \max}$ and $T_{\max}$ were determined from the obtained stresses using the well known formulae of the strength of materials.

Table 5

$\eta = 3.2992$					
σ/τ	$T_{\max}$	$M_{b\ \max}$	$\tau_{b\ \max}$	$\sigma_{b\ \max}$	m
0	2970	0	199	0	2
0.2	2902	304	195	39	2
0.4	2767	579	186	74	3
0.6	2740	861	184	110	3
0.8	2656	1112	178	143	3
1.0	2513	1316	169	169	3
1.25	2388	1563	160	200	3/4
1.667	2187	1909	147	245	3
2.5	1701	2227	114	286	3
5.0	945	2473	63	317	3
∞	0	2789	0	358	4

7. Final remarks

The aim of this study, which was to develop a method for analysis of the stability of thin-walled orthotropic rods with various shapes of the cross-sections, subject to complex loads (compression, bending, torsion) has been achieved. The obtained values of the critical loads of thin-walled rods with closed cross-sections and with at least one axis of symmetry overlapping the bending plane of the rods, have proved to be accurate enough for engineering calculations, which entitles the authors to extend this method to the analysis of post-critical states in the future.

The development of the computer algorithm for various widths, thicknesses and material (orthotropic) properties of individual plate strips will allow for optimisation of the structure with respect to its stability.

The presented analysis of the influence of the number of rod walls with the cross- section in the form of a regular polygon, subject to simultaneous bending and torsional deflection, on its stability (values of critical loads and buckling

modes) shows that one can calculate shell and plate structures (composed of sections of cylindrical shells and plates) with this method as well.

References

1. BENITO R., SRIDHARAN S., 1985, Interactive Buckling Analysis with Finite Strips, *Int. J. Num. Math. Engng.*, **21**, 146-161
2. BIDERMANN B.L., 1977, *Mechanics of Thin-Walled Structures – Static*, Moscow (in Russian)
3. BISKUPSKI J., KOŁAKOWSKI Z., 1994, Stability of Thin-Walled Box Girders Subjected to Bounded Torsion, *Engineering Machines Problems*, **3**, 3, 57-72
4. COLLADINI C.R., 1973, A Plastic Theory for Collapse of Plate Girders under Combined Shearing Force and Bending Moment, *Structural Engineer*, **S1**, 147-154
5. EVANS H.R., POSTER D.M., ROCKEY K.C., 1978, The Collapse Behaviour of Plate Girders Subjected to Shear and Bending, *Proc. Inst. Assn. Bridge and Struct. Eng.*, **P-18/78**, 1-20
6. GRAVES-SMITH T.R., SRIDHARAN S., 1978, A Finite Strip Method for the Buckling of Plate Structures under Arbitrary Loading, *Int. J. Mech. Sci.*, **20**, 685-693
7. HARDING J.E., HOBBS R.E., NEAL B.G., 1977, Ultimate Load Behaviour of Plates under Combined Direct and Shear in Plane Loading, Steel Plates Structures, Sypmosium (eds. Dowling, Harding and Frieze) Crosby Lockwood, 369-403
8. KRÓLAK M. (edit.), 1990, *Post-Buckling Behaviour and Load Carrying Capacity of Thin-Walled Plate Girders*, PWN, Warsaw-Łódź, (in Polish)
9. KRÓLAK M. (edit.), 1995, *Stability, Post-Buckling Behaviour and Load Carrying Capacity of Thin, Orthotropic Flat-Walled Structures*, Technical University of Lodz, (in Polish)
10. KRÓLAK M., KOŁAKOWSKI Z., 1987, The Post-Buckling State of the Thin-Walled Trapezoidal Girders, Loaded by a Normal Force and a Bending Moment, *Archiwum Budowy Maszyn*, **XXXIV**, 2, 143-158
11. LAN S.C., HANCOCK G.J., 1983, Buckling of Thin Flat-Walled Structures by Spline Finite Strip Method, *Proc. Inst. Civ. Engns.*, Part 1, **75**, 311-323
12. MURRAY N.W., 1973, Buckling of Stiffened Panels Loaded Axially and in Bending, *Struct. Engineer*, **S1**, 2, 285-301

13. PLANK R.J., WITTRICK W.H., 1974a, Buckling under Combined Loading of Thin, Flat-Walled Structures by a Complexfinite Strip Method, *Int. J. Num. Meth. Engng.*, **8**, 323-339

14. PLANK R.J., WITTRICK W.H., 1974b, Critical Buckling of Some Stiffened Panels in Compression, Shear, and Bending, *Aeronautical Quaterly*, 165-179

15. PROTTE W., 1976, Zur Beulung Versteifter Kastenträger Mit Symmetrischem Trapez - Querschnitte unter Biegemomenten-, Normalkraft-, und Querkraftbeanspruchung, *Tech. Mitt. Krupp-Forsch*, Berlin, A2, **34**

16. SRIDHARAN S., GRAVES-SMITH T.R., 1981, Postbuckling Analysis with Finite Strips, *J. of Engng. Mech. Div., ASCE.*, **107**, EM5, 869-888

17. STROUD W.J., GREENE W.H., ANDERSON M.S., 1989, Buckling Loads of Stiffened Panels Subjected to Combined Longitudinal Compression and Shear: Results Obtained with PASCO, EAL and STAGS Computers Programs, *NASA TP-2215*, January

18. STURM R.G., 1947, Stability of Thin Cylindrical Shells in Torsion, *Proc. Am. Soc. Civil Eng.*, **73**, 4, 471-495

19. WOLMIR A.S., 1967, *Ustoichivost deformiruemykh system*, Izd. "Nauka", Moskwa

Stateczność i nośność cienkościennych ortotropowych słupów o przekroju wielokąta foremnego poddanego obciążeniom złożonym

Streszczenie

W pracy przeprowadzono analizę stateczności i nośności granicznej cienkościennych ortotropowych prętów (słupów, belek, masztów, wałów), których przekrój poprzeczny jest wielokątem foremnym, poddanych obciążeniom złożonym (ściskanie, zginanie, skręcanie). Zagadnienie stateczności (stan krytyczny) rozwiązano asymptotyczną metodą Byskova-Hutchinsona biorąc pod uwagę pierwszy rząd przybliżenia. Sprawdzenie poprawności wyników dotyczących stateczności (obciążeń krytycznych i postaci wyboczenia) oraz obliczenia nośności granicznej przeprowadzono metodą elementów skończonych, wykorzystując pakiet MES ANSYS 5.4. Wyniki obliczeń przedstawiono w postaci wykresów. W oparciu o otrzymane wyniki sformułowano szereg wniosków i uwag końcowych.

Manuscript received November 15, 2000; accepted for print January 24, 2001